Ultrafast dynamics of nonequilibrium electrons in metals under femtosecond laser irradiation

B. Rethfeld*
Institut für Laser- und Plasmaphysik, Universität Essen, D-45117 Essen, Germany

A. Kaiser
Max-Planck-Institut für Physik komplexer Systeme, Nöthnitzer Straße 38, D-01187 Dresden, Germany

M. Vicanek and G. Simon
Institut für Theoretische Physik, TU Braunschweig, D-38106 Braunschweig, Germany
(Received 5 December 2001; revised manuscript received 21 March 2002; published 22 May 2002)

Irradiation of a metal with an ultrashort laser pulse leads to a disturbance of the free-electron gas out of thermal equilibrium. We investigate theoretically the transient evolution of the distribution function of the electron gas in a metal during and after irradiation with a subpicosecond laser pulse of moderate intensity. We consider absorption by inverse bremsstrahlung, electron-electron thermalization, and electron-phonon coupling. Each interaction process is described by a full Boltzmann collision integral without using any relaxation-time approach. Our model is free of phenomenological parameters. We solve numerically a system of time- and energy-dependent integro-differential equations. For the case of irradiation of aluminum, the results show the transient excitation and relaxation of the free-electron gas as well as the energy exchange between electrons and phonons. We find that laser absorption by free electrons in a metal is well described by a plasmalike absorption term. We obtain a good agreement of calculated absorption characteristics with values experimentally found. For laser excitations near damage threshold, we find that the energy exchange between electrons and lattice can be described with the two-temperature model, in spite of the nonequilibrium distribution function of the electron gas. In contrast, the nonequilibrium distribution leads at low excitations to a delayed cooling of the electron gas. The cooling time of laser-heated electron gas depends thus on excitation parameters and may be longer than the characteristic relaxation time of a Fermi-distributed electron gas depending on internal energy only. We propose a definition of the thermalization time as the time after which the collective behavior of laser-excited electrons equals the thermalized limit.

DOI: 10.1103/PhysRevB.65.214303 PACS number(s): 63.20.Kr, 05.20.Dd, 42.50.Ct

I. INTRODUCTION

Nonequilibrium dynamics of the electron gas in metals irradiated by ultrashort laser pulses has been an area of intense research during the last couple of decades. With the advent of femtosecond laser pulses, direct experimental studies of fundamental processes such as electron-electron scattering and electron-phonon interaction in metals have become possible.[1–14]

Nonequilibrium between electrons and phonons is important already on a picosecond time scale. In a metal, first, free electrons absorb energy from the laser while the lattice remains cold. On a femtosecond time scale the energy is distributed among the free electrons by electron-electron collisions leading to the thermalization of the electron gas. The energy exchange between electrons and the lattice is governed by electron-phonon collisions. Though the electron-phonon collision time τ_{ep} may be as short as the electron-electron collision time τ_{ee},[15] the energy transfer from the hot electrons to the lattice will last much longer than the thermalization of the electron gas due to the large mass difference of electrons and phonons; typically a few tens of picoseconds. This picture was widely verified experimentally.[1–4,16,17] It is described by the classical two-temperature model,[18,19] assuming that electron distributions and phonon distributions can be characterized in terms of electron temperature T_e and lattice temperature T_p, respectively. Then the energy exchange is given by

$$c_p \frac{\partial T_p}{\partial t} = -c_e \frac{\partial T_e}{\partial t} = \alpha (T_e - T_p), \tag{1}$$

where c_e and c_p are the specific heats of electrons and phonons, respectively. The energy exchange rate α between electrons and the lattice is related to the electron-phonon coupling constant.[20,21] The validity range of the two-temperature model is obviously limited to times longer than the electron-electron collision time τ_{ee}, lying in the femtosecond range. However, as will be discussed below, there are doubts about its validity on time scales up to 1 ps.

In metals electron-electron scattering acts on femtosecond time scales. This result was obtained by probing the lifetime of laser-excited electrons in two-photon photoemission experiments.[9,10,22] As soon as an electron is excited to an energy ε above Fermi energy $\varepsilon_{\mathrm{Fermi}}$, it will decay after a time $\tau_{ee} \propto (\varepsilon - \varepsilon_{\mathrm{Fermi}})^{-2}$.[23,24] However, the distribution function of electrons is in nonequilibrium for a much longer time because secondary electrons are created. Thus, many electron-electron collisions are needed to establish finally a Fermi distribution. It was shown experimentally that the electron distribution function, after excitation with a femtosecond laser pulse, is not in thermal equilibrium for a few 100 fs up to the picosecond regime.[5,7] Theoretical calculations confirm a nonequilibrium of the electron gas on this time scale.[15,25] Thus, the description of the electron gas with a temperature T_e as done in the two-temperature model (1) is questionable for time scales below 1 ps.

When investigating nonequilibrium dynamics of electron gases in metals, one fundamental question is the mutual influence of electron-electron interaction and electron-phonon interaction. For low excitations, experiments on gold and silver have shown a delay of electron-phonon relaxation compared with the prediction of the two-temperature model. This effect was attributed to a nonthermalized electron gas.[11–14]

Theoretical studies are essential to model the dynamics of a laser-excited electron gas and to understand the consequence of a nonthermalized electron gas in metals. Whether and when a distribution function may be assumed to be thermalized, strongly depends on the features one wishes to observe. When studying electron emission, for example, one is only interested in high-energy electrons. Then it is sufficient to focus on the high-energy tail of the distribution function and on the lifetime of one electron, which is the time an electron stays in the high-energy region. Since the electron-electron collision time depends on the electron energy, this lifetime is much shorter than the collision time of an electron in the low-energy region. However, low-energy electrons are essential when investigating the time needed to establish a Fermi distribution, which is important for the collective behavior of the free-electron gas. The transient evolution of the electron distribution in metals after laser excitation is thus of fundamental interest for a wide field of research.

In this work we investigate the nonequilibrium dynamics of electrons in metals irradiated with a laser pulse of moderate intensity, where the electron gas is significantly disturbed but no lattice damage occurs. We use a time- and energy-dependent kinetic description, applying Boltzmann collision integrals explicitly without any relaxation-time approximation, thus, without preanticipating any feature of the system's way of relaxation to equilibrium. In other investigations published so far [7,12,15,25,26,14] different approaches are used to model the energy absorption, the electron-phonon interaction, and the electron-electron interaction While the latter is mostly calculated using a detailed collision term,[7,27] electron-phonon collisions are usually described by a relaxation-time approach. For modeling the energy absorption strength, different phenomenological collision rates are applied. Now we present, to the best of our knowledge, the first calculation of the temporal evolution of the electron distribution function in laser-excited metal representing each process by a detailed collision integral. Neither relaxation-time approaches nor phenomenological parameters are applied in our calculations. Therefore, since we do not make any preassumptions about the behavior of the electrons, we are able to observe any unexpected behavior of the nonequilibrium electron gas. Our results show the transient evolution of the distribution function of the laser-excited electron gas. To interpret the calculated dynamics of the distribution function of the laser-excited electron gas we focus on the consequence of the nonequilibrium found. According to our results, after strong excitation even a nonequilibrium electron gas may *behave* as if it were in a Fermi distribution, and, therefore, its energy exchange with lattice may be described by Eq. (1). However, if the electron gas is only slightly excited, the energy exchange between electrons and lattice is delayed compared with Eq. (1) and the two-temperature model fails. We thus confirm the experimental results of Refs. 11–14. Our detailed microscopical model gives a clear explanation for the delayed energy exchange between the weakly excited electron gas and the lattice. Finally, we propose a definition of the thermalization time of the laser-excited electron gas after which its collective behavior equals the behavior of a Fermi-distributed electron gas.

In the following section we introduce the applied model and the collision integrals used for the numerical calculation. Section III explains the numerical algorithm and the adaptation of the model to a specific material. As an example, we calculate the distribution functions in the free-electron-like metal aluminum. The resulting electron dynamics is presented in Sec. IV, where the evolution of the nonequilibrium distribution function is shown. We compare the calculated energy absorption with known absorption characteristics. The energy exchange between electrons and lattice is investigated for high and low excitations. We determine the thermalization time of a laser-excited electron gas as a function of excitation strength.

II. THEORETICAL MODEL

We assume a perfect, homogeneous, and isotropic material. The laser shall have a moderate intensity that is sufficiently large to disturb the free-electron gas significantly but is not so high that lattice damages may occur. We neglect energy transport as well as spatial variation of pulse intensity. This can be interpreted as the irradiation of a thin film of metal. Corresponding to our assumption of homogeneity and isotropy we take an average over all polarization directions of the incident laser light. We are aware that these assumptions are simplifications of the real situation, however, our intention is to reveal some universal features of the *transient* excitation and relaxation dynamics of electrons and phonons in a metal. Therefore, we focus on the time-dependent behavior of the distribution functions, believing that our results are fairly general. With our simplifications, the model is spatially independent and the distribution functions depend only on time and the modulus of the momentum or, equivalently, on time and energy.

In order to consider photon absorption by inverse bremsstrahlung, electron-electron interaction, and electron-phonon interaction, one collision integral is used for each listed process. None of these complete collision integrals will be approximated by a relaxation-time approach. Moreover, any phenomenological parameters are avoided in our calculation. Thus, even the dynamics of a highly nonequilibrium electron distribution is described by our model. The phonon gas shall be affected only by the electron gas directly. Therefore, energy absorption by the lattice directly from the laser as well as phonon-phonon collisions are neglected.

In total this yields to a system of Boltzmann's equations for the distribution function of the electron gas, $f(k)$, and of the phonons gas, $g(q)$, which read

$$\frac{\partial f(k)}{\partial t} = \left.\frac{\partial f(k)}{\partial t}\right|_{\text{el-el}} + \left.\frac{\partial f(k)}{\partial t}\right|_{\text{el-phon}} + \left.\frac{\partial f(k)}{\partial t}\right|_{\text{absorb}}, \quad (2)$$

$$\left.\frac{\partial g(q)}{\partial t}=\frac{\partial g(q)}{\partial t}\right|_{\text{phon-el}}. \tag{3}$$

Here, the distribution functions $f(k)$ and $g(q)$ depend on the modulus of the wave vectors of electrons, $\boldsymbol{k}$ and phonons, $\boldsymbol{q}$, respectively. Before irradiation, $f(k)$ is assumed to be a Fermi-Dirac distribution and $g(q)$ shall be a Bose-Einstein distribution, both at room temperature.

In the following we will have a closer look at the considered interaction processes and their collision terms occurring in Eqs. (2) and (3).

A. Electron-electron collisions

Electron-electron collisions lead to an energy relaxation within the electron gas called thermalization. Through this process the absorbed energy is distributed among the free electrons so that the electron gas tends towards a thermal equilibrium and thus to a Fermi distribution.

The collision term that describes the electron-electron interaction is given by[7,27]

$$\begin{aligned}\left.\frac{\partial f(k)}{\partial t}\right|_{\text{el-el}}=&\frac{2\pi}{\hbar}\sum_{\boldsymbol{k}_1}\sum_{\boldsymbol{k}_2}|M_{ee}(\Delta k)|^2\delta(\varepsilon(k_3)+\varepsilon(k_1)-\varepsilon(k_2)\\&-\varepsilon(k))[f(k_3)f(k_1)\{1-f(k)\}\{1-f(k_2)\}\\&-f(k)f(k_2)\{1-f(k_3)\}\{1-f(k_1)\}],\end{aligned} \tag{4}$$

where $\Delta\boldsymbol{k}=\boldsymbol{k}_1-\boldsymbol{k}_2=\boldsymbol{k}-\boldsymbol{k}_3$ is the exchanged momentum and the wave vector $\boldsymbol{k}_3$ results from momentum conservation. $\varepsilon(k)$ is the energy of an electron with the modulus of the wave vector k. The matrix element M_{ee} is derived from a screened Coulomb potential $M_{ee}\propto(\Delta k^2+\kappa_{\text{sc}}^2)^{-1}$, where κ_{sc} is the static screening length. This screening length represents an important parameter for the electron-electron interaction and is calculated at each time step for the current distribution function $f(k)$ according to Ref. 28,

$$\kappa_{\text{sc}}^2=\frac{e^2m_e}{\pi^2\hbar^2\varepsilon_0}\int_0^\infty f(k)dk. \tag{5}$$

Here, m_e is the effective mass of a free electron in the conduction band. Using Eq. (5), the screening length κ_{sc} is consistently calculated even for a highly nonequilibrium electron gas.

B. Electron-phonon collisions

The main effect of electron-phonon collisions is to transfer energy from the laser-heated electron gas to the cold lattice. By emission of phonons the electron gas cools down. Since the maximum phonon energy is small compared to the kinetic electron energy, one electron-phonon collision changes the energy of the electron gas only slightly. Thus, many electron-phonon collisions are necessary to decrease the amount of kinetic energy stored in the electron gas. In addition, electron-phonon interactions have an equilibration effect on the electron gas. Phonon emission and absorption occur in such a way that the electron gas tends to establish a Fermi distribution (at phonon temperature).

The collision term for the electron-phonon interaction reads[21,29]

$$\begin{aligned}\left.\frac{\partial f(k)}{\partial t}\right|_{\text{el-phon}}=&\frac{2\pi}{\hbar}\sum_{\boldsymbol{q}}|M_{\text{el-phon}}(q)|^2\{\delta(\varepsilon(k^+)-\varepsilon(k)\\&-\varepsilon_{\text{ph}}(q))[f(k^+)\{1-f(k)\}\{g(q)+1\}-f(k)\\&\times\{1-f(k^+)\}g(q)]+\delta(\varepsilon(k^-)-\varepsilon(k)\\&+\varepsilon_{\text{ph}}(q))[f(k^-)\{1-f(k)\}g(q)\\&-f(k)\{1-f(k^-)\}\{g(q)+1\}]\},\end{aligned} \tag{6}$$

where $\boldsymbol{k}^+=\boldsymbol{k}+\boldsymbol{q}$ and $\boldsymbol{k}^-=\boldsymbol{k}-\boldsymbol{q}$ are the wave vectors of an electron with resulting or initial wave vector $\boldsymbol{k}$ before or after emission or absorption of a phonon with wave vector $\boldsymbol{q}$ respectively. $\varepsilon_{\text{ph}}(q)$ is the energy of a phonon with the modulus of wave vector q.

In metals, not only the interaction of one electron with the lattice deformation has to be taken into account but also the screening of the lattice deformation by free electrons[30,31] and the interaction of that electron with the screening electrons.[24] This is considered by the electron-phonon matrix element $M_{\text{el-phon}}(q)$ given in Ref. 32 with $|M_{\text{el-phon}}(q)|^2\propto\varepsilon_{\text{ph}}(q)(q^2+\kappa_{\text{sc}}^2)^{-1}$. The electron screening length κ_{sc} is given above by Eq. (5).

C. Energy absorption

Energy absorption from the laser occurs in a metal mainly through free electrons. In the classical picture, a free electron oscillates in the electromagnetic field of the laser and absorbs energy only when it is changing its momentum parallel to the oscillation direction. This can happen through a third collision partner, which disturbs the oscillation of the electron. The kinetic oscillation energy is $\langle\epsilon_{\text{kin}}\rangle=e^2E_L^2/(4m_e\omega_L^2)$ on average, where ω_L is the angular frequency of the laser light and E_L is the amplitude of its electric field. In our case, we consider laser irradiation with parameters of such magnitude that the average kinetic energy of an oscillating electron $\langle\epsilon_{\text{kin}}\rangle$ is much less than the photon energy $\hbar\omega_L$. Therefore, the absorption has to be described in quanta of photons rather than by classical absorption.[33] Analogously to the classical picture, a third collision partner is also needed in the quantum-mechanical one in order to ensure energy and momentum conservation.

In the literature, two collision integrals for absorption and emission of photons by free electrons can be found. The first one was given by Épshtein.[34] He used second quantization to derive a collision term that describes the absorption of photons by free electrons in the conduction band of an insulator when colliding with phonons. For this case, photon absorption mediated by electron-phonon collisions leads to good agreement of our calculations with experiments.[35] Seely and Harris[36] derived such a collision term of photon absorption for inverse bremsstrahlung in a plasma, which differs from the expression of Épshtein only by the mediating matrix element of the three-particle interaction. In metals the largest contribution to absorption is mediated by electron-ion collisions,[37,38] as in a plasma. Therefore, we apply the ex-

pression of Seely and Harris to model the photon absorption by free electrons. With laser light of frequency ω_L and amplitude of electric field $\boldsymbol{E}_L$, this electron-photon-ion collision term reads

$$\left.\frac{\partial f(k)}{\partial t}\right|_{\text{absorb}} = \frac{2\pi}{\hbar}\sum_{\Delta k}|M_{\text{el-ion}}(\Delta k)|^2 \sum_l J_l^2\left(\frac{e\boldsymbol{E}_L\cdot\Delta\boldsymbol{k}}{m_e\omega_L^2}\right) \times[f(k')\{1-f(k)\}-f(k)\{1-f(k')\}]\delta(\varepsilon(k') -\varepsilon(k)+l\hbar\omega_L). \quad (7)$$

Here $\Delta\boldsymbol{k}$ is the exchanged momentum, and $\boldsymbol{k}'=\boldsymbol{k}+\Delta\boldsymbol{k}$ is the resulting or initial wave vector of the colliding electron.

For the electron-ion interaction we assume again a screened Coulomb potential like for electron-electron collisions, which yields the same matrix element, see Sec. II A. The probability of absorption (or emission) of l photons is given by the square of the Bessel function J_l^2. The product $\boldsymbol{E}_L\cdot\Delta\boldsymbol{k}$ in the argument of the Bessel function only allows absorption of a photon if the change of the electron wave vector $\Delta\boldsymbol{k}$ has a component *parallel* to the electric laser field $\boldsymbol{E}_L$. This is analogous to the classical description. Because we do not consider a particular polarization of the laser light, an average is made over all directions of $\boldsymbol{E}_L$. In our calculations electric laser field amplitudes $\boldsymbol{E}_L$ of such magnitude are assumed so that the argument of the Bessel function J_l^2 is always small compared to unity. Therefore, the probability of multiphoton processes with $|l|>1$ is much smaller than that of one-photon processes. Preliminary calculations have shown that multiphoton processes can be neglected within the considered range of laser parameters.

At first glance, the consideration of ions as well as phonons in our model may appear surprising. However, it is a consistent description since in our model metal electrons are considered as *free* electrons, such as those in a plasma rather than Bloch electrons. Therefore, the interaction of electrons with fixed ions has to be included separately. This can be understood when looking at the Hamiltonian of the metal,

$$\mathcal{H}=\sum_j \frac{\hbar^2}{2m_e}\boldsymbol{k}_j^2+\sum_{j,\alpha} V(\boldsymbol{r}_j-\boldsymbol{R}_\alpha)+\mathcal{H}_{ee}+\mathcal{H}_{ii}, \quad (8)$$

where the first term describes the energy of the free electrons, the second term denotes the interaction of electrons at positions $\boldsymbol{r}_j$ with ions at positions $\boldsymbol{R}_\alpha$, and the third and fourth terms denote the electron-electron interaction and the ion-ion interaction, respectively. The second term is usually expanded, leading to a term describing the interaction of electrons with fixed ions and the interaction of electrons with the potential caused by the displacement $\delta\boldsymbol{R}_\alpha$ of ions from their equilibrium positions $\boldsymbol{R}_{\alpha,0}$:

$$\mathcal{H}=\sum_j \frac{\hbar^2\boldsymbol{k}_j^2}{2m_e}+\sum_{j,\alpha} V(\boldsymbol{r}_j-\boldsymbol{R}_{\alpha,0})-\sum_{j,\alpha}\delta\boldsymbol{R}_\alpha\nabla V(\boldsymbol{r}_j-\boldsymbol{R}_{\alpha,0}) +\mathcal{H}_{ee}+\mathcal{H}_{ii}. \quad (9)$$

The first two terms of Eq. (9) are usually combined to Bloch electrons, while the third term describes the electron-phonon interaction. In our work, however, we describe the electrons as *free* electrons, thus we consider only the first term of Eq. (9). The second term of Eq. (9), i.e. the interaction of electrons with fixed ions, should therefore be considered seperately. This separation does not affect the standard electron-phonon interaction, described by the third term in Eq. (9). Note that collisions of electrons with *fixed* ions change solely the *momentum* of free electrons, while the *energy* of a free electron changes in collisions with ion *vibrations*, which are represented by phonons. Thus, in our model, electron-ion collisions mediate the energy absorption of laser light by free electrons, while energy transfer between the electron gas and lattice occurs through electron-phonon interaction.

We consider only one dispersion relation of free electrons, thus only intraband absorption mechanisms are possible. In polyvalent materials, also interband absorption between nearly parallel bands may play a role.[39–41] In contrast to intraband absorption, interband absorption occurs without momentum transfer to the absorbing electron. This absorption mechanism, associated with bound electrons rather than with free electrons,[39] is neglected in our model.

D. Equation for phonons

The phonon distribution function is assumed to change only due to phonon-electron collisions. Direct absorption of the laser energy is neglected. For simplicity, we consider only one phonon mode and do not take umklapp processes into account. Thus, phonon-phonon collisions are neglected as well. Phonon-electron interaction leads to heating of the phonon gas, analogously to the cooling of the electron gas by electron-phonon collisions, see Sec. II B.

The phonon-electron collision term is given by

$$\left.\frac{\partial g(q)}{\partial t}\right|_{\text{phon-el}} = 2\frac{2\pi}{\hbar}|M_{\text{phon-el}}(q)|^2\sum_{\boldsymbol{k}}\delta(\varepsilon(k^+)-\varepsilon(k) -\varepsilon_{\text{ph}}(q))[f(k^+)\{1+g(q)\}\{1-f(k)\} -g(q)f(k)\{1-f(k^+)\}] \quad (10)$$

with $\boldsymbol{k}^+=\boldsymbol{k}+\boldsymbol{q}$. The matrix element $M_{\text{phon-el}}$ is the same as the matrix element $M_{\text{el-phon}}$, described in Sec. II B.

III. NUMERICAL SOLUTION

In this section we give an overview of how and with which assumptions the equation system with the above introduced collision terms is numerically solved. First the collision sums are transformed into collision integrals using the common approaches, so we are dealing with one sixfold integral and three threefold integrals. Due to the assumed isotropy, the integrals can be analytically reduced to a single twofold integral and three one-fold integrals, respectively, which depend only on the modulus of the electron and phonon wave vectors.[27,35,42]

The energy dispersion of electrons is approximated by a parabola, $\varepsilon(k)=\hbar^2k^2/2m_e$, with the effective electron mass m_e. For phonons, Debye's dispersion relation is assumed,

$\varepsilon_{\mathrm{ph}}(q)=v_s q$, where v_s is the speed of sound. Then, the system of nonlinear integro-differential equations (2) and (3) and the collision integrals can be rewritten depending on time and energy, using the distribution function $f(\varepsilon(k),t)$ and $g(\varepsilon_{\mathrm{ph}}(q),t)$.

In order to solve the equation system numerically, discrete electron energies and phonon energies are considered, resulting in a system of about 250 fully coupled, nonlinear ordinary differential equations. The integration over time is done by applying Runge-Kutta integration of fifth order with automatic step-size control.[43] With this procedure, we are able to follow the time evolution of the distribution functions $f(\varepsilon(k),t)$ and $g(\varepsilon_{\mathrm{ph}}(q),t)$ and observe their changes due to excitation of the electron gas by the laser beam, thermalization of the electron gas by electron-electron collisions, and energy exchange between the electron gas and phonon gas due to electron-phonon collisions.

While in metals the assumption of Debye's dispersion relation for phonons is not really a restriction, the parabolic dispersion for the electrons is. However, in aluminum the electrons dispersion relation resembles rather well a free-electron-like parabolic dispersion relation; therefore we chose aluminum for our calculations. Other dispersion relations could also be included, but this would make the calculations more demanding. Gold is often chosen for similar calculations, however, in gold there are *d*-band electrons about 2.5 eV below the Fermi edge of the free *s* electrons, requiring much more complicated calculations: These *d* electrons cannot be neglected even for lasers with $\hbar\omega_L < 2.5$ eV, since during irradiation free states occur below the Fermi edge (see Sec. IV A) and, therefore, the *d* electrons may also be strongly excited.

For the calculation of the time evolution of the distribution functions in a given material, here aluminum, several parameters have to be provided. These are the free-electron density $n_e=18.0\times10^{28}\ \mathrm{m}^{-3}$, the wave number at Fermi energy for $T_e=0$ K, $k_{F,0}=(3\pi^2 n_e)^{1/3}=1.747\times10^{10}\ \mathrm{m}^{-1}$, the ion density $n_i=n_e/3$, and Debye's wave number $q_{\mathrm{Debye}}=(6\pi^2 n_i)^{1/3}=1.526\times10^{10}\ \mathrm{m}^{-1}$.[44,45] The effective electron mass m_e and the speed of sound v_s are needed for the dispersion relations. We calculated the internal energy of electrons and phonons for different temperatures T_e and T_p, respectively, and compared the resulting heat capacities with experimental values.[42] This leads to an effective electron mass of $m_e=1.45m_{e,\mathrm{free}}$ for aluminum, as also derived in Ref. 46. The phonon heat capacity turned out to be best reproduced when applying the sound speed of longitudinal phonons, $v_s=v_{s,\mathrm{long}}=6260$ m/s.[45] Note that all these parameters describe the *undisturbed* crystal. No parameters describing the investigated dynamics of the electron gas and phonon gas or the interaction with the laser beam are introduced. Neither do any phenomenological parameters or fit parameters occur in our calculations.

IV. RESULTS FOR ALUMINUM

We assume a laser pulse of constant intensity with duration $\tau_L=100$ fs and vacuum wavelength $\lambda=630$ nm, corresponding to a photon energy of $\hbar\omega_L=1.97$ eV $=0.245\varepsilon_{\mathrm{Fermi}}$. Electrons and phonons are assumed to be initially in thermal equilibrium at 300 K.

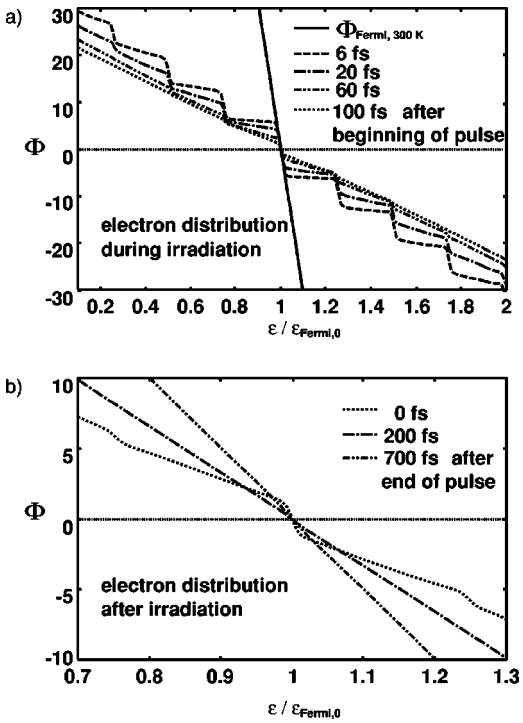

FIG. 1. Distribution function of free electrons in aluminium (a) during and (b) after irradiation. The quantity $\Phi(f)$ defined by Eq. (11) is shown as a function of electron energy. A laser pulse of 100 fs duration with constant intensity was assumed with a photon energy of $\hbar\omega_L=1.97$ eV $=0.245\varepsilon_{\mathrm{Fermi}}$ and an electric-field amplitude $E_L=1.4\times10^8$ V/m. (b) shows a section of about $\varepsilon_{\mathrm{Fermi}}\pm\hbar\omega_L$ of the energy scale.

A. Change of electron distribution function

Figure 1 shows the transient behavior of the occupation number of free electrons for an electric laser field of amplitude $E_L=1.4\times10^8$ V/m, corresponding to an intensity of $I_L=7\times10^9$ W/cm^2 and an absorbed fluence of $F_{\mathrm{abs}}=0.7$ mJ/cm^2. A function Φ, which is defined as

$$\Phi(f(\varepsilon)) := -\ln\left(\frac{1}{f(\varepsilon)}-1\right), \tag{11}$$

is shown as a function of electron energy $\varepsilon/\varepsilon_{\mathrm{Fermi},0}$. This function increases monotonically with increasing occupation number $f(\varepsilon)$ and is particularly suitable to visualize the perturbation of the electron gas. In thermal equilibrium, when electrons obey a Fermi-Dirac distribution, $\Phi(\varepsilon)$ equals $(\varepsilon_{\mathrm{Fermi},0}-\varepsilon)/(k_B T_e)$. In this case, $\Phi(\varepsilon)$ is a linear function with a slope proportional to the inverse electron temperature $1/T_e$. Thus, a deviation of the electron gas from thermal equilibrium is directly reflected in a deviation of $\Phi(\varepsilon)$ from a straight line. Figure 1(a) shows a strong perturbation of the electron gas immediately after the beginning of irradiation. In comparison with the straight solid line representing the initial Fermi distribution at 300 K, the absorption of photons lead to a steplike distribution function: Electrons below

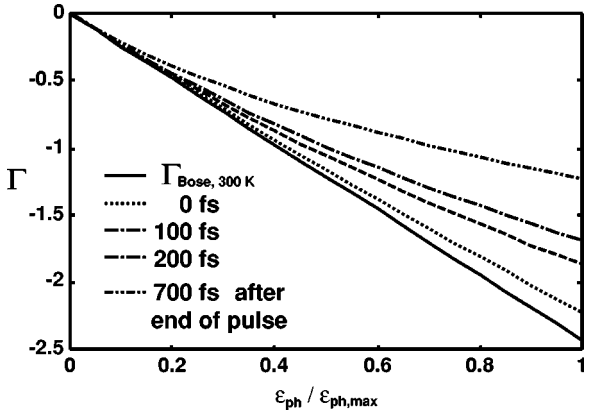

FIG. 2. Distribution function of phonons for the same laser parameters as in Fig. 1. The function $\Gamma(g) = -\ln(1+1/g)$ of the distribution function g is shown in dependence on phonon energy, where the maximum phonon energy $\varepsilon_{\text{ph, max}} = \hbar q_{\text{Debye}}$.

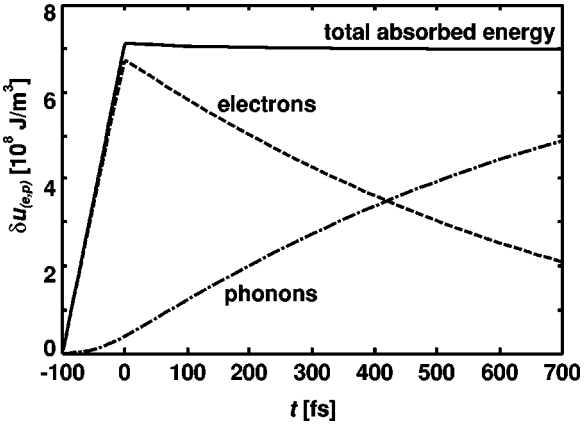

FIG. 3. Transient energy increase of electron gas, δu_e, and of phonon gas, δu_p, respectively, and total absorbed energy δu. The laser pulse was assumed with the same parameters as in Fig. 1.

Fermi energy absorb photons, leading to an increase of the occupation number of electrons with energies up to $\hbar\omega_L$ above Fermi energy. An excited electron may absorb a further photon, leading to an increase of the occupation number for energies up to $2\hbar\omega_L$ above Fermi energy. The occupation number of electrons below Fermi energy decreases at the same rate, reproducing the Fermi edge in steps of $\hbar\omega_L$. A similar steplike electron distribution function was found for energies above the Fermi energy in Refs. 47 and 48, including also one step below the Fermi energy. Experimentally the first plateau of excited electrons with energies up to $\varepsilon_{\text{Fermi}} + \hbar\omega_L$ was observed in gold in Refs. 5 and 6, and theoretically reproduced in Refs. 15 and 25. Our logarithmlike plot of the function $\Phi(\varepsilon)$ has the advantage that not only excited electrons above Fermi energy but also the resulting ''holes'' below Fermi energy are easily observed. In Fig. 1(a) the evolution of the electron distribution function during irradiation is shown. The clear steplike structure at the beginning of the pulse is washed out quickly due to electron-electron collisions, which act towards thermal equilibrium within the electron gas and smoothen the function $\Phi(\varepsilon)$. Figure 1(b) shows the completion of electron thermalization after irradiation for energies of about $\pm\hbar\omega_L$ around the Fermi edge. A straight line $\Phi(\varepsilon)$, corresponding to a Fermi distribution $f_{\text{Fermi}}(\varepsilon)$, is reached about 200 fs after irradiation has ended; its slope, however, is still much smaller than those for the Fermi distribution at 300 K. Thus the electron gas is heated significantly. Later on, the effect of electron-phonon interaction is also visible. The cooling of the hot electron gas leads to an increasing slope of $\Phi(\varepsilon)$, corresponding to lower electron temperatures.

B. Change of phonon distribution function

Figure 2 shows the change of the distribution function of the phonons due to electron-phonon interaction. A function Γ, defined as $\Gamma(g(\varepsilon_{\text{ph}})) := -\ln[1+1/g(\varepsilon_{\text{ph}})]$, is shown, which is a linear function with a slope proportional to $1/T_p$ in thermal equilibrium, when phonons obey a Bose-Einstein distribution.

The phonon gas is nearly unaffected during the pulse. After irradiation ends, the occupation number and thus the inherent energy of the phonon gas increases. Since the matrix element of phonon-electron interaction vanishes for $\varepsilon_{\text{ph}} \to 0$, the phonon distribution function becomes slightly equilibrium shifted at later times.

In the following we focus on electron and phonon behavior during and directly after irradiation, where the disturbance of phonons from thermal equilibrium can be neglected.

C. Absorption characteristics

The internal energy within the electron gas, $u_e(t)$, or phonon gas, $u_p(t)$, is calculated by integrating over the corresponding distribution functions $f(k,t)$ and $g(q,t)$, respectively. Due to the assumption of isotropy, this reads for the electrons $u_e(t) = 2/2\pi^2 \int_0^\infty f(k,t)\hbar^2k^2/(2m_e)k^2dk$.

The gain of additional internal energy due to laser excitation in the electron gas at time t, $\delta u_e(t)$, is given by the difference between $u_e(t)$ and the initial energy $u_e(-\infty)$. Since we assumed the free electrons to be initially in thermal equilibrium at a temperature of 300 K, for the absorbed energy of the electron gas, $\delta u_e(t)$ follows

$$\delta u_e(t) := u_e(t) - u_e(-\infty) = \frac{2}{2\pi^2}\int_0^\infty [f(k,t) - f_{\text{Fermi,300 K}}(k)]\frac{\hbar^2k^2}{2m_e}k^2dk. \quad (12)$$

Here, $f_{\text{Fermi,300 K}}$ is the Fermi-Dirac distribution at room temperature (300 K). Analogously, the gain of absorbed energy per volume by phonons $\delta u_p(t) := u_p(t) - u_p(-\infty)$ is calculated keeping in mind that initially the phonons are in Bose-Einstein distribution at a temperature of 300 K. The sum of both increments of internal energy, $\delta u(t) = u_e(t) + u_p(t)$, gives the total energy absorbed from the laser. Checking whether $\delta u(t)$ remains constant after irradiation can be used to verify the numerical stability of our calculations.

Figure 3 shows the transient behavior of energy increase for the electron gas, the phonon gas, and the total absorbed

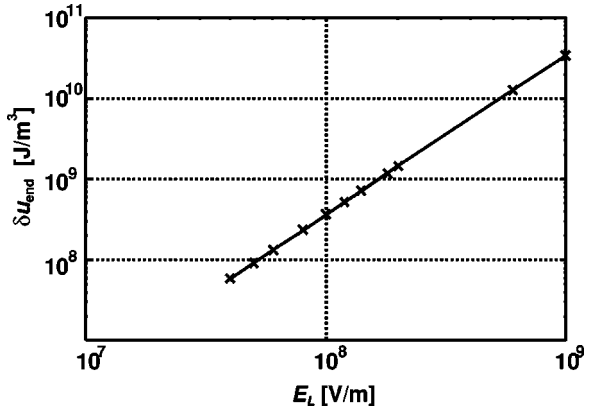

FIG. 4. Total absorbed energy δu_{end} as a function of electric laser field E_L. A laser pulse of 100 fs duration, $\lambda = 630$ nm, and constant electric field was assumed.

energy, respectively, for the same laser parameters as in Fig. 1. The absorbed energy $\delta u(t)$ increases linearly during irradiation with constant intensity, as expected. After irradiation δu remains constant at a value $\delta u_{\mathrm{end}} := \delta u(\infty)$, in this case $\delta u_{\mathrm{end}} = 7.1 \times 10^8$ J/m^3.

We applied a wide range of electric laser field amplitudes E_L, respective of laser intensities I_L. For all laser intensities considered up to damage threshold, the absorbed energy δu increases linearly during irradiation with constant intensity, thus the energy increase can be expressed as $du/dt = \delta u_{\mathrm{end}}/\tau_L$. As shown in Fig. 4, the absorbed energy after irradiation δu_{end} is proportional to the square of the electric laser field E_L^2, and hence proportional to the laser intensity I_L. Since, compared with spatially dependent absorption characteristics, the equation $dI/dz = -du/dt$ and thus for our case $dI/dz \propto I$ holds, the absorption characteristics in our calculations correspond to the usual exponential absorption profile $I(z) = I_L \exp(-\mu z)$. The absorption strength in our calculations can thus be compared with literature by extracting the corresponding absorption constant $\mu = -I(z)^{-1} dI/dz|_z$, which for $z = 0$ in our case equals $\mu = I_L^{-1} \delta u_{\mathrm{end}}/\tau_L$. The intensity I_L inside the material is given by the density of the energy flux of an electromagnetic wave in metal, $I_L = \sqrt{\epsilon_0/\mu_0}\, n E_L^2$,[49] where n is the real part of the complex refractive index. In aluminum n equals 1.36 for $\lambda = 630$ nm.[50] From Fig. 3, we find that the calculated absorption strength corresponds to an absorption constant of $\mu_{\mathrm{num}} = 1.01 \times 10^8$ m^{-1}. The experimental value for aluminum for $\lambda = 630$ nm is $\mu_{\mathrm{Lit}} = 1.52 \times 10^8$ m^{-1}.[50] However, in aluminum absorption is to a large extent caused by interband processes, not considered in our model. At the applied photon energy, intraband absorption provides about the sixth part of the total absorption.[40,41] Thus, our calculated absorption strength appears to be larger than the expected intraband absorption strength. We also performed calculations with a higher photon energy at $\lambda = 350$ nm, where interband absorption is less pronounced. In this case, the calculated absorption strength is $\mu_{\mathrm{num}} = 1.1 \times 10^8$ m^{-1},[42] in good comparison with the literature value of $\mu_{\mathrm{Lit}} = 1.54 \times 10^8$ m^{-1}.[50]

Thus, keeping in mind that no phenomenological parameter entered our calculation, the calculated absorption strength compares well with literature. The comparison confirms the validity of our applied absorption term developed in Sec. II C. Note that we did not consider spatial variation of the electric laser field in our calculations but used known experimental spatial absorption characteristics only for comparison with our calculations. The comparison refers to the qualitative dependence of absorption on laser intensity and to the quantitative absorption strength.

D. Energy relaxation between electrons and phonons

In Fig. 3 the energy increase in the electron gas $\delta u_e(t)$ and the energy increase in the phonon gas δu_p are shown together with the total absorbed energy δu during and after irradiation with a laser pulse specified in Fig. 1. The energy increase in the electron gas during irradiation follows the total absorbed energy with a slight decrease due to energy transfer to the phonon gas during the pulse. After irradiation has ended, energy transfer from the electron gas to the phonon gas continues. The electron gas loses energy at the same rate as the phonon gas is heated up. This process, caused by electron-phonon collisions, continues until both systems have the same temperature. Because of the large difference in heat capacity, this corresponds to a much lower internal energy of the electron gas δu_e than of the phonon gas δu_p.

When aluminum is irradiated by a 100-fs laser pulse with a constant electric-field amplitude of $E_L = 1.4 \times 10^8$ V/m (intensity $I_L = 7 \times 10^9$ W/cm^2), the electron gas absorbs an amount of energy of $\delta u_e = 6.7 \times 10^8$ J/m^3. If this electron gas was to thermalize without energy loss, i.e., with constant internal energy, it would end in a Fermi-Dirac distribution at a temperature of $T_e = 3215$ K. An interesting question is how the cooling behavior of the laser-excited electron gas differs from that of a Fermi-distributed electron gas with the same internal energy. The cooling of both, the laser-excited electron gas as well as the corresponding Fermi-distributed electron gas, is shown in Fig. 5(a). According to this figure, the energy transfer rates from both kinds of electron gas to the phonon gas are essentially the same. This implies that for these relatively high laser intensities the energy exchange between free electrons and phonons is determined by the internal energy δu_e only, which can be characterized by a temperature T_e, and can thus be described by the two-temperature model (1). The electron-phonon coupling constant α in Eq. (1) can be extracted from Fig. 5(a). We find a value of $\alpha = 310 \times 10^{15}$ J/K s m^3 for aluminum.

In the case of irradiation with a smaller intensity, e.g., by a 100-fs laser pulse with an electric laser field amplitude of $E_L = 4 \times 10^7$ V/m (laser intensity of $I_L = 5.8 \times 10^8$ W/cm^2), the two-temperature model does not hold, see Fig 5(b). In this case, the electron gas is excited more weakly than in Fig. 5(a); it has absorbed an energy of $\delta u_e = 5.5 \times 10^7$ J/m^3. A Fermi distribution at $T_e = 960$ K has the same internal energy. Figure 5(b) shows that the initial cooling rate of the laser-heated electron gas is substantially lower than the cooling rate of the corresponding Fermi-distributed electron gas. Such delay of energy transfer to the lattice for a laser perturbed electron gas compared with the two-temperature model was observed experimentally at low temperatures and

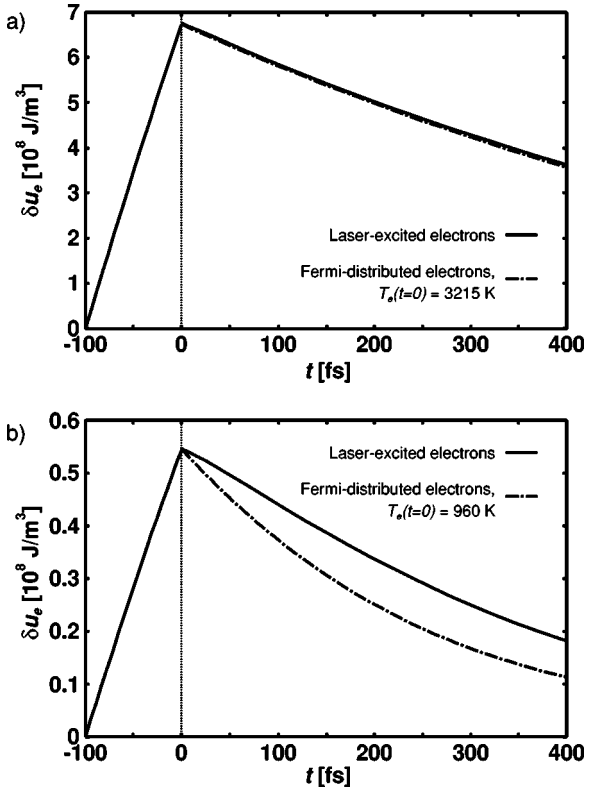

FIG. 5. Transient internal energy of laser excited electron gas (solid lines) for excitation with a laser-pulse of 100 fs duration and a constant electric-field amplitude of (a) $E_L=1.4\times10^8$ V/m (intensity $I_L=7\times10^9$ W/cm^2) and (b) $E_L=4\times10^7$ V/m (intensity $I_L=5.8\times10^8$ W/cm^2). The dashed-dotted lines show the cooling of a corresponding Fermi-distributed electron gas, which has the same internal energy at the time $t=0$.

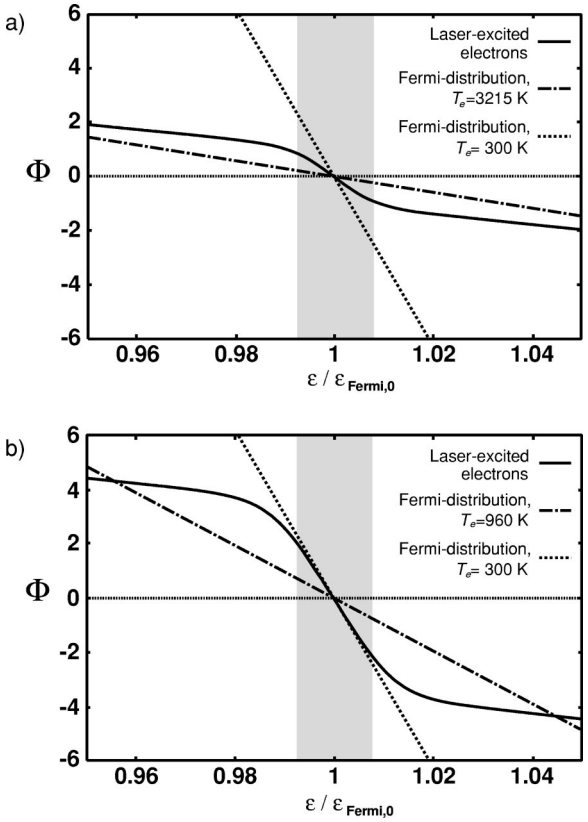

FIG. 6. Distribution function of laser-excited electron gas (solid lines) for excitation with a laser pulse of 100 fs duration and a constant electric-field amplitude of (a) $E_L=1.4\times10^8$ V/m (intensity $I_L=7\times10^9$ W/cm^2) and (b) $E_L=4\times10^7$ V/m (intensity $I_L=5.8\times10^8$ W/cm^2). The quantity $\Phi(f)$, defined by Eq. (11) is shown as a function of electron energy. The dashed-dotted lines show the corresponding Fermi-distributed electron gas, which has the same internal energy as the laser-excited electron gas. The dotted lines show the Fermi distribution for an electron gas at room temperature. A region of one maximum phonon energy around the Fermi edge is shaded.

for very low intensities.[11–14] Thus, for weak excitation, the cooling rate of the laser-heated electron gas is determined by its particular electron distribution function in nonequilibrium and not only by the internal energy as in the case of stronger excitation.

In order to explain this different behavior, we have plotted in Figs. 6(a) and 6(b) the above-mentioned electron distributions near the Fermi edge at a time when the laser pulse has just ended ($t=0$ in Fig. 5). The functions Φ of the distribution functions given by Eq. (11) are shown near the Fermi edge. In Fig. 6(a) Φ is shown for an electron gas after laser excitation with a field of $E_L=1.4\times10^8$ V/m, leading to an absorbed energy of $\delta u_e=6.7\times10^8$ J/m^2. The function Φ of a Fermi-distributed electron gas with $T_e=3215$ K, having the same internal energy, and with $T_e=300$ K are shown as well. The same was done in Fig. 6(b) for the electron gas excited by a laser pulse with $E_L=4\times10^7$ V/m, which causes an energy increase of $\delta u_e=5.5\times10^7$ J/m^3. Also Φ of the corresponding Fermi distribution with $T_e=960$ K and $\Phi(f_{\mathrm{Fermi,\,300\,K}})$ are plotted in Fig. 6(b).

At $t=0$ the hot electron gas interacts with a phonon gas of about $T_p\simeq300$ K. Thus, at this moment the electron-phonon interaction acts on the electron gas in such a way that the electron gas tries to establish a Fermi distribution at 300 K. To this end, electrons above Fermi energy have to be transferred to states below Fermi energy. However, due to the small phonon energy, the phonons are able to act on the electrons only in a small region around the Fermi edge. The maximum phonon energy in the case of aluminum is about $0.008\ \varepsilon_{\mathrm{Fermi}}$.

In Fig. 6(b) the distribution functions in the case of low excitation are shown. In the region of one maximum phonon energy around Fermi energy (shaded area), the laser-excited electron gas shows nearly no deviation from the Fermi distribution at 300 K. In contrast, the Fermi distribution with $T_e=940$ K of a thermalized electron gas with the same internal energy differs strongly from the Fermi distribution at 300 K. Thus, after low exitation, the phonon cooling of the nonequilibrium electron gas is much less efficient than the cooling of a corresponding thermalized Fermi-distributed electron gas. Therefore, the cooling rates are far from being the same, which explains the different slopes of energy decay at $t=0$ in Fig. 5(b).

In contrast, for high excitations as shown in Fig. 6(a), the distribution function of the laser-excited electron gas devi-

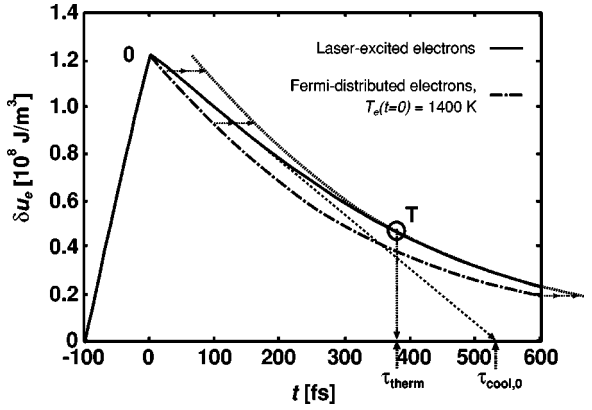

FIG. 7. Determination of the cooling time $\tau_{\mathrm{cool},0}$ and the thermalization time τ_{therm}. The example is shown for the case of irradiation with a 100-fs laser pulse with an electric-field amplitude of $E_L = 6 \times 10^7$ V/m. The cooling time is extracted through the slope of energy decrease (dashed line) directly after excitation ($t=0$, point O). The thermalization time is found by shifting the cooling curve of the Fermi-distributed electron gas keeping constant energy (dotted line) until from a certain point T onwards, both cooling curves coincide.

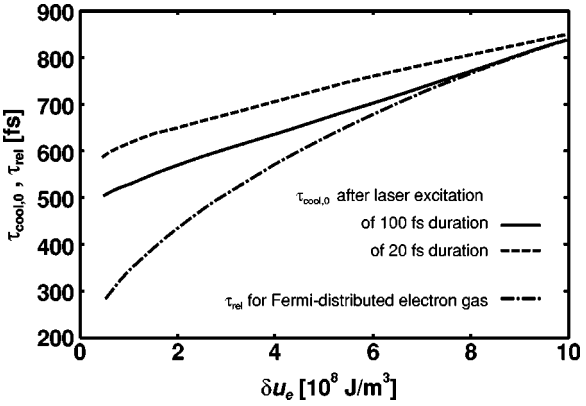

FIG. 8. Cooling time $\tau_{\mathrm{cool},0}$ of nonequilibrium electron gas after excitation with a laser pulse of constant intensity and duration of 100 fs (solid line) and 20 fs (dashed line) depending on internal energy, together with the relaxation time τ_{rel} of the corresponding Fermi-distributed electron gas (dashed-dotted line).

ates strongly from the Fermi distribution at 300 K in the region of one maximum phonon energy. In this case the cooling of the laser-excited electron gas by phonon emission is nearly as efficient as the cooling of the Fermi-distributed electron gas. Though also here the distribution function of the laser-excited electron gas differs from the corresponding Fermi distribution, i.e., the electron gas has a highly nonequilibrium distribution function, our calculations show that its *cooling behavior* is nearly the same as the behavior of a thermalized electron gas.

E. Relaxation time and thermalization time for electrons

The so-called relaxation time is a characteristic time for the energy exchange between the electron gas and phonon gas. Yet, when speaking about relaxation time τ_{rel}, equilibrium states and only those transitions that run through equilibrium states are considered. In this case, τ_{rel} is a general feature of the heated electron gas, which depends only on the internal energy or temperature of the electron gas. In our case the time for energy exchange depends strongly on pulse characteristics and thus on the history of the electron gas. Therefore, we prefer to speak about an ''initial cooling time'' $\tau_{\mathrm{cool},0}$, which characterizes the energy decrease directly after the pulse. We extract it from our calculations through the slope of the energy decrease of the electron gas after irradiation has ended, see Fig. 7.

Figure 8 shows the cooling times $\tau_{\mathrm{cool},0}$ of the electron gas in aluminum as a function of the internal energy. To demonstrate the dependence of the cooling time $\tau_{\mathrm{cool},0}$ on the history of the electron gas, we assumed excitations with a laser pulse of 20 fs and 100 fs duration, respectively, and a constant intensity. The internal energy was adjusted by using different laser intensities. Furthermore, the relaxation time τ_{rel} of a corresponding Fermi-distributed electron gas of the same internal energy is shown. We see that the energy transfer between the laser-excited electron gas and lattice is delayed for small excitations and short pulse lengths. The dependence on excitation strength was discussed in Sec. IV D; the dependence on laser-pulse duration is evident, since for longer pulses electron-electron interaction already works towards a thermalized electron gas during the pulse.

Although an excited electron gas in equilibrium and in nonequilibrium acts differently in detail, its macroscopic *behavior*, in particular, the cooling behavior, is not distinguishable after a specific time. In Figs. 5(b) and 7 we see that as time proceeds, the rate of electron cooling (slope of the curve) of the laser-excited electron gas becomes equal to the cooling rate of the Fermi-distributed electron gas, compared at the same energy. This provides an opportunity to define a new value to characterize the electron gas. For this, we introduce the thermalization time τ_{therm}, which gives the time when an electron gas in nonequilibrium exchanges energy with a cold lattice at the same rate as a Fermi-distributed electron gas, which has the same internal energy. Figure 7 shows graphically how the thermalization time τ_{therm} is extracted from our calculations. Note that this is *not* the time after which a Fermi distribution is established but the time at which the laser-excited electron gas *behaves* as a Fermi-distributed electron gas. The behavior of the laser-excited electron gas may be the same as the behavior of the Fermi-distributed electron gas *before* an equilibrium is reached in the laser-excited electrons.

Figure 9 shows the thermalization time of the laser-excited electron gas depending on internal energy after irradiation with a laser pulse of constant intensity and a duration of 20 fs and 100 fs, respectively. The thermalization time τ_{therm} after an excitation of 100 fs duration is about 80 fs shorter than the τ_{therm} for a 20-fs excitation because in this case the electron gas is already thermalizing during irradiation.

V. CONCLUSIONS

We investigated irradiation of metals with a femtosecond laser pulse using a kinetic description. The effects of particu-

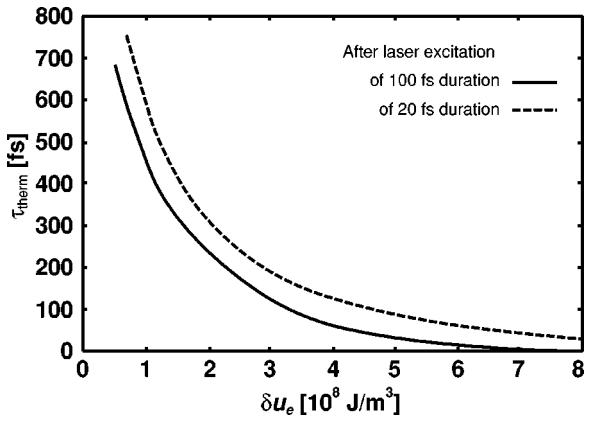

FIG. 9. Thermalization time τ_{therm} of nonequilibrium electron gas after excitation with a laser pulse of constant intensity and duration of 100 fs (solid line) and 20 fs (dashed line) depending on internal energy. τ_{therm} is defined as the time when the cooling rate of the laser-excited electron gas equals the cooling rate of a corresponding Fermi-distributed electron gas, see Fig. 7.

lar collision processes on the electron distribution function were studied. In our model we consider absorption by inverse bremsstrahlung, electron-electron thermalization, and electron-phonon coupling. In contrast to other kinetic approaches[7,12,15,25,26,14] we explicitly calculate the transient free-electron distribution by microscopic collision integrals, avoiding any phenomenological or averaging parameters and without using any relaxation-time approach. In this way, we are able to follow the transient evolution of a laser-excited electron gas even when it is in a highly nonequilibrium state, without anticipating any feature of its behavior.

We solve a system of time- and energy-dependent Boltzmann equations numerically for the free-electron-like metal aluminum. The results show in detail the transient excitation and thermalization of the free-electron gas as well as the energy exchange between electrons and phonons. The total absorbed energy was calculated for different laser intensities and compares well with absorption characteristics known from literature. For excitations near damage threshold, we found that the nonequilibrium electron gas does not affect the electron-phonon interaction and the energy exchange can be described by the two-temperature model. In contrast, for lower excitations, the energy transfer from electron gas to lattice is influenced by the nonequilibrium of the laser-excited electron gas. In this case, the cooling of the electron gas is delayed compared to a thermalized electron gas of the same internal energy, which is in agreement with earlier experimental results.[11–14] The reason is that the distribution function of a weakly excited electron gas shows only a very slight deviation from an electron gas at room temperature in the region around the Fermi edge. The calculated electron cooling time thus depends on excitation parameters and may be longer than the characteristic relaxation time of a Fermi-distributed electron gas, which depends on internal energy only. To characterize this, we defined an electron thermalization time as the time after which the collective behavior of the laser-excited electron gas is the same as the behavior of a corresponding Fermi-distributed electron gas. Note that also the thermalization time depends on laser parameters.

We are grateful to S.I. Anisimov, K. Sokolowski-Tinten, and D. von der Linde for valuable suggestions and helpful discussions. This work was supported in part by the Deutsche Forschungsgemeinschaft under Grant No. Si 158/13.

*Electronic address: brf@ilp.physik.uni-essen.de

[1] J. G. Fujimoto, J. M. Liu, E. P. Ippen, and N. Bloembergen, Phys. Rev. Lett. **53**, 1837 (1984).
[2] H. E. Elsayed-Ali T. B. Norris, M. A. Pessot, and G. A. Mourou, Phys. Rev. Lett. **58**, 1212 (1987).
[3] R. W. Schoenlein, W. Z. Lin, J. G. Fujimoto, and G. L. Eesley, Phys. Rev. Lett. **58**, 1680 (1987).
[4] S. D. Brorson, A. Kazeroonian, J. S. Moodera, D. W. Face, T. K. Cheng, E. P. Ippen M. S. Dresselhaus, and G. Dresselhaus, Phys. Rev. Lett. **64**, 2172 (1990).
[5] W. S. Fann, R. Storz, H. W. K. Tom, and J. Bokor, Phys. Rev. B **46**, 13 592 (1992).
[6] W. S. Fann, R. Storz, H. W. K. Tom, and J. Bokor, Phys. Rev. Lett. **68**, 2834 (1992).
[7] C.-K. Sun, F. Vallée, L. H. Acioli, E. P. Ippen, and J. G. Fujimoto, Phys. Rev. B **50**, 15 337 (1994).
[8] X. Y. Wang, D. M. Riffe, Y.-S. Lee, and M. C. Downer, Phys. Rev. B **50**, 8016 (1994).
[9] C. A. Schmuttenmaer, M. Aeschlimann, H. E. Elsayed-Ali, R. J. D. Miller, D. A. Mantell, J. Cao, and Y. Gao, Phys. Rev. B **50**, 8957 (1994).
[10] T. Hertel, E. Knoesel, M. Wolf, and G. Ertl, Phys. Rev. Lett. **76**, 535 (1996).
[11] R. H. M. Groeneveld, R. Sprik, and A. Lagendijk, Phys. Rev. B **45**, 5079 (1992).
[12] R. H. M. Groeneveld, R. Sprik, and A. Lagendijk, Phys. Rev. B **51**, 11 433 (1995).
[13] N. Del Fatti, R. Bouffanais, F. Vallee, and C. Flytzanis, Phys. Rev. Lett. **81**, 922 (1998).
[14] N. Del Fatti, C. Voisin, M. Achermann, S. Tzortzakis, D. Christofilos, and F. Vallee, Phys. Rev. B **61**, 16 956 (2000).
[15] D. Bejan and G. Raseev, Phys. Rev. B **55**, 4250 (1997).
[16] G. L. Eesley, Phys. Rev. B **33**, 2144 (1986).
[17] M. B. Agranat, S. I. Anisimov, S. I. Ashitkov, B. I. Makshantsev, and I. B. Ovchinnikova, Fiz. Tverd. Tela (Leningrad) **29**, 3267 (1987) [Sov. Phys. Solid State **29**, 1875 (1987)].
[18] S. I. Anisimov, A. M. Bonch-Bruevich, M. A. El'yashevich, Y. A. Imas, N. A. Pavlenko, and G. S. Romanov, Zh. Tekh. Fiz. **36**, 1273 (1966) [Sov. Phys. Tech. Phys. **11**, 945 (1967)].
[19] S. I. Anisimov, B. L. Kapeliovich, and T. L. Perel'man, Zh. Eksp. Teor. Fiz. **66**, 776 (1974) [Sov. Phys. JETP **39**, 375 (1974)].
[20] M. I. Kaganov, I. M. Lifshitz, and L. V. Tanatarov, Zh. Eksp. Teor. Fiz. **31**, 232 (1956) [Sov. Phys. JETP **4**, 173 (1957)].
[21] P. B. Allen, Phys. Rev. Lett. **59**, 1460 (1987).
[22] M. Aeschlimann, M. Bauer, S. Pawlik, W. Weber, R. Burgermeister, D. Oberli, and H. C. Siegmann, Phys. Rev. Lett. **79**, 5158 (1997).
[23] L. D. Landau and E. M. Lifschitz, *The Classical Theory of Fields*, Course of Theoretical Physics Vol. 2 (Pergamon Press, Oxford, 1962).
[24] D. Pines and P. Nozieres, *Normal Fermi Liquids*, The Theory of

Quantum Liquids Vol. I (Addison-Wesley, New York, 1966).
[25] A. V. Lugovskoy and I. Bray, Phys. Rev. B **60**, 3279 (1999).
[26] V. E. Gusev and O. B. Wright, Phys. Rev. B **57**, 2878 (1998).
[27] D. W. Snoke, W. W. Rühle, Y.-C. Lu, and E. Bauser, Phys. Rev. B **45**, 10 979 (1992).
[28] R. Binder, H. S. Köhler, M. Bonitz, and N. Kwong, Phys. Rev. B **55**, 5110 (1997).
[29] J. M. Ziman, *Electrons and Phonons* (Clarendon Press, Oxford, 1962).
[30] J. Bardeen, Phys. Rev. **52**, 688 (1937).
[31] J. M. Ziman, *Electrons and Phonons* (Oxford University Press, 1962).
[32] N. Ashcroft and N. Mermin, *Solid State Physics* (Saunders College Publishing, 1976).
[33] Y. B. Zel'dovich and Y. P. Raĭzer, Zh. Eksp. Teor. Fiz. **47**, 1150 (1964) [Sov. Phys. JETP **20**, 772 (1965)].
[34] E. M. Épshtein, Fiz. Tverd. Tela (Leningrad) **11**, 1787 (1970) [Sov. Phys. Solid State **11**, 2213 (1970)].
[35] A. Kaiser, B. Rethfeld, M. Vicanek, and G. Simon, Phys. Rev. B **61**, 11 437 (2000).
[36] J. F. Seely and E. G. Harris, Phys. Rev. A **7**, 1064 (1973).
[37] W. Rozmus, V. T. Tikhonchuk, and R. Cauble, Phys. Plasmas **3**, 360 (1996).
[38] D. F. Price, R. M. More, R. S. Walling, G. Guethlein, R. L. Shepherd, R. E. Stewart, and W. E. White, Phys. Rev. Lett. **75**, 252 (1995).
[39] H. Ehrenreich, H. R. Philipp, and B. Segall, Phys. Rev. **132**, 1918 (1963).
[40] N. W. Ashcroft and K. Sturm, Phys. Rev. B **3**, 1898 (1971).
[41] B. Huettner, J. Phys.: Condens. Matter **6**, 2459 (1994).
[42] B. Rethfeld, Ph.D. thesis, Technische Universität Braunschweig, 1999.
[43] W. H. Press and S. A. Teukolsky, *Numerical Recipes in C* (Cambridge University Press, New York, 1992).
[44] C. Kittel, *Introduction to Solid State Physics* (Wiley, New York, 1956).
[45] I. S. Grigorev and E. Z. Mejlikhov, *Fizicheskie Velichini* (Energoatomizdat, Moscow, 1991).
[46] N. W. Ashcroft and J. W. Wilkins, Phys. Lett. **14**, 285 (1965).
[47] A. V. Lugovskoy, T. Usmanov, and A. V. Zinoviev, J. Phys. D **27**, 623 (1994).
[48] A. V. Lugovskoy, T. Usmanov, and A. V. Zinoviev, J. Opt. Soc. Am. B **15**, 53 (1998).
[49] L. D. Landau and E. M. Lifschitz, *Electrodynamics of Continuous Media*, Course of Theoretical Physics Vol. 8 (Pergamon Press, Oxford, 1960).
[50] E. Palik, *Handbook of Optical Constants in Solids* (Academic Press, London, 1997).